AMERICAN JOURNAL OF BIOCHEMISTRY AND BIOTECHNOLOGY

RESEARCH ARTICLE

Accumulation and Effect of Manganese on Chloroplasts and Antioxidant Responses in Arabidopsis Thaliana

Jun Xing, Xue Yang, Cailing Yuan*

Drug Research and Development Center, Shandong Drug and Food Vocational College, Weihai, Shandong, China

*Corresponding Author: yuancailing12345@163.com

Abstract: In this study, 5-day-old seedlings of *Arabidopsis thaliana* were exposed to 0, 0.5, and 1.0 mmol/L $MnCl_2$ for 6 days by using three independent biological replicates. The results indicated that Mn content in roots exhibited a dose-dependent increase with rising external Mn supply. The elevated Mn levels led to significant reductions in the nutrient content of K, Ca, Na, and Fe in roots. In addition, exposure to 0.5 and 1.0 mmol/L Mn decreased the content of chlorophyll. Both 0.5 and 1.0 mmol/L Mn decreased chlorophyll fluorescence intensity as observed by confocal microscopy. The activities of catalase, superoxide dismutase, and peroxidase were reduced by 0.5 and 1.0 mmol/L Mn in roots. The treatment with 0.5 and 1.0 mmol/L Mn led to a substantial accumulation of malondialdehyde (MDA) and H_2O_2. In contrast, the reduced glutathione (GSH) content exhibited an opposite trend. Moreover, Mn exposure decreased the mitochondrial membrane potential ($\Delta\Psi m$) but increased the fluorescence of reactive oxygen species in root cells by laser scanning confocal microscopy. In summary, this study highlights that Mn toxicity impairs photosynthesis, disrupts antioxidant defenses, and induces oxidative damage in the seedlings of *Arabidopsis thaliana*.

Keywords: Manganese, Chlorophyll, Antioxidant Enzyme, Reactive Oxygen Species, Root

Received: 19-07-2025 | **Revised:** 13-02-2026 | **Accepted:** 03-03-2026 | **DOI:** 10.3844/ajbbsp.2026.22.01.028

Introduction

Manganese (Mn) is one of the essential nutrients that plays a critical role in plant development and growth [1, 2]. One of its most important functions in photosystem II is serving as a key component of the oxygen-evolving complex, where it is indispensable for photosynthetic electron transport and water oxidation [3, 4]. Accordingly, Mn deficiency severely impairs photosynthesis, leading to chlorosis and thylakoid membrane disorganization [5]. It has been found that Mn deficiency reduces chlorophyll content by impairing key biosynthesis enzyme Mg-chelatase in Pinus sylvestris [6, 7].

Nevertheless, excess Mn is a toxic element to plants. A main toxicity mechanism is the induction of oxidative stress via the induction of Reactive Oxygen Species (ROS) [8-10]. Plants respond by activating antioxidant defenses, including Mn-dependent superoxide dismutase (SOD) and glutathione (GSH) [11, 12]. Interestingly, moderate Mn stress can enhance antioxidant enzyme activities such as peroxidase (POD) and catalase (CAT) [13, 14], but this protective response often fails under higher Mn concentrations [15, 16].

In addition, the plants have developed a sophisticated mechanism to regulate Mn homeostasis [17-19]. Previously, several Mn-responsive genes have been identified by transcriptomic analyses, including metal transporters and ROS-scavenging enzymes [20]. Despite significant progress in understanding Mn homeostasis, the results of field studies show that Mn toxicity symptoms vary significantly among different crop species and cultivars [21]. Moreover, how Mn excess simultaneously affects chlorophyll metabolism in leaves and antioxidant responses in roots within a short-term exposure period has not been fully elucidated. For the dual role of Mn in plant physiology, the effects of Mn on the metabolism of chlorophyll and antioxidant systems need to be studied. In the current study, the effect of Mn homeostasis on the metabolism of chlorophyll and antioxidant systems was examined. By integrating physiological and biochemical perspectives, our results will provide a comprehensive framework for understanding Mn dynamics in plants and developing strategies to improve plant resilience to Mn imbalance.

Materials and Methods

Plant Cultivation

Arabidopsis thaliana Columbia ecotype (Col-0) seeds were sterilized with 75% ethanol and 5% sodium hypochlorite for 2 min each, and washed three times with sterile water. After vernalization at 4°C for 2 days, approximately 30 seeds were sown per Petri dish (90 mm diameter) on Murashige and Skoog (MS) medium with 1% sucrose and 0.8% agar (pH adjusted to 5.8). The plants were cultivated under conditions of 22°C, a 12-h photoperiod, and a light intensity of 120 μmol/(m²·s) for 5 days. Subsequently, we transferred uniform seedlings to fresh MS medium with 0, 0.5, and 1.0 mmol/L $MnCl_2$ for 6 days, respectively. There were three replicates for each treatment. Roots and leaves were then sampled for physiological and biochemical analyses. In the whole experiment, environmental factors including temperature, light, and humidity were strictly controlled as part of the standardized growth protocol in this study.

Analyzing the Content of Chlorophyll

The leaves were carefully weighed and pooled to ensure sufficient sample quantity for analysis. Chlorophyll content was assayed with the acetone extraction method. Briefly, the leaf samples were finely chopped and completely submerged in an 80% acetone solution to facilitate chlorophyll extraction. To prevent photodegradation of chlorophyll, we put the samples in the dark for 48 h at room temperature, allowing for complete pigment dissolution. After extraction, the supernatant was obtained by centrifugation for 10 min at 4,000 rpm to remove tissue debris. The extracted solution was then detected at 645 nm and 663 nm with a UV spectrophotometer (SPECTRA MAX M5, Molecular Devices). Chlorophyll a and chlorophyll b concentrations were acquired according to the following equations [22]:

1) Chlorophyll-a = 12.72 A663 - 2.59 A645
2) Chlorophyll-b = 22.88 A645 - 4.67 A663

Detecting Chlorophyll Fluorescence by Laser Scanning Confocal Microscopy

Fresh leaves were sampled from seedlings after the 6-day treatment period. The leaves were gently washed with pH 7.0 Phosphate-Buffered Saline (PBS) to remove surface contaminants and immediately prepared for microscopy to preserve in vivo chlorophyll integrity. Each leaf was mounted flat on a pre-cleaned glass slide with the upper surface facing the objective lens. A drop of PBS was added to prevent tissue dehydration during observation, and a coverslip was gently placed on top without applying pressure to avoid cellular damage.

Chlorophyll fluorescence images were obtained with a confocal microscope (Leica TCS SP2) and an argon-ion laser source. For chlorophyll excitation, the laser wavelength was set to 488 nm. Prior to sample imaging, the system was calibrated using control leaf samples to optimize laser power and Photomultiplier Tube (PMT) gain. These settings were kept constant across all experimental groups to enable comparative analysis of fluorescence intensity. For each treatment group, three optical fields were captured per leaf. Image acquisition parameters (pinhole size, scan speed, and frame averaging) were standardized to ensure consistent spatial resolution and signal-to-noise ratio across all samples.

Analyzing the Activity of Antioxidant Enzymes

Fresh root samples were carefully weighed (~ 0.1 g) and rapidly frozen in liquid nitrogen to preserve enzymatic activity. The tissues were then homogenized in pre-chilled 1.5 mL microcentrifuge tubes using a sterile pestle, with 1 mL of ice-cold

50 mM PBS (pH 7.8, containing 0.1 mM EDTA and 1% polyvinylpyrrolidone) added as the extraction buffer. The homogenate was centrifuged for 10 min at 3,000 r/min and 4°C to pellet cellular debris. Supernatant was immediately put into new tubes and kept on ice for subsequent enzymatic assays. Enzyme activities were determined using colorimetric commercial assay kits (Nanjing Jiancheng Bioengineering Institute, China) strictly according to the manufacturer's instructions. All assays were performed in triplicate for each sample. Absorbance readings were obtained using a microplate reader (SPECTRA MAX M5, Molecular Devices).

Analyzing the Level of ROS and GSH Content

The supernatant obtained from root samples during antioxidant enzyme analysis was further utilized for the quantification of ROS and GSH levels. The level of ROS and GSH content was assayed in the supernatant. The content of malondialdehyde (MDA), H2O2, and GSH was detected with the kits purchased from Nanjing Jiancheng Bioengineering Institute (Nanjing, China). The concentration of MDA was detected with the thiobarbituric acid (TBA) method. H_2O_2 content was measured via a peroxidase-coupled reaction. The content of glutathione was assayed based on its reaction with 5,5'-dithiobis-(2-nitrobenzoic acid) (DTNB), and GSH reduces DTNB to produce 2-nitro-5-thiobenzoic acid (TNB), which yields a yellow color measurable at 412 nm.

Analyzing ROS in Roots by Laser Scanning Confocal Microscopy

To visualize general ROS accumulation in Arabidopsis roots, the fluorescent probe 2',7'-dichlorodihydrofluorescein diacetate (H_2DCFH-DA, 10 μM) was used. H_2DCFH-DA is a cell-permeable indicator that becomes fluorescent upon oxidation by intracellular ROS, producing a fluorescent compound, 2',7'-dichlorofluorescein (DCF). Freshly harvested roots were incubated in 10 μM H_2DCFH-DA (dissolved in PBS, pH 7.4) in the dark for 30 min at 25°C to prevent premature oxidation. After incubation, roots were gently rinsed three times with PBS (5 min per wash) to remove excess extracellular probe and minimize background fluorescence. Roots were briefly blotted on filter paper to remove residual liquid before imaging. A confocal microscope (Leica TCS SP2, Germany) was used for fluorescence detection with 488 nm excitation and emission collection range 500-550 nm (green channel). Prior to sample imaging, the system was calibrated using control root samples to optimize laser power and photomultiplier tube (PMT) gain. These settings were kept constant across all experimental groups to enable comparative analysis of fluorescence intensity.

Analyzing the Fluorescence of Mitochondrial Membrane Potential in Roots by Laser Scanning Confocal Microscopy

The mitochondrial membrane potential (ΔΨm) in root cells was assessed using the potential-sensitive cationic fluorescent dye Rhodamine 123. For the assay, freshly harvested roots were immersed in a 10 μM solution of Rhodamine 123 (prepared in pH 7.4 PBS) and incubated for 30 minutes at 25°C in complete darkness to prevent photobleaching. Following incubation, roots were gently rinsed three times with fresh PBS (5 minutes per wash) to thoroughly remove any non-specifically bound or extracellular dye. Fluorescence imaging was performed immediately using a confocal microscope (Germany) equipped with an argon-ion laser. Rhodamine 123 was excited at a wavelength of 488 nm, and its fluorescence emission was acquired within the 500-550 nm range (typically displayed in a yellow channel). Prior to sample imaging, the system was calibrated using control root samples to optimize laser power and photomultiplier tube (PMT) gain. These settings were kept constant across all experimental groups to enable comparative analysis of fluorescence intensity.

Analyzing Mineral Nutrition Elements

The root samples were carefully rinsed with deionized water to remove surface contaminants prior to analysis. For elemental determination, approximately 0.1 g of dried root tissue was subjected to microwave-assisted acid digestion in Teflon vessels using 10 mL HNO_3 as the digestion medium. Following complete digestion, the resulting solution was diluted with deionized water to 10 mL. The concentrations of elements were subsequently detected by an inductively coupled plasma sector field mass spectrometry (ICP-SF-MS; Agilent, Japan).

Data Analysis

Results were expressed as mean ± standard deviation (SD). Statistical analyses of the effects of Mn treatment on chlorophyll content, ROS levels, GSH content, and antioxidant enzyme activities were conducted using SPSS 16.0 (IBM Corporation, USA). Differences among groups were evaluated using one-way analysis of variance (ANOVA), followed by

post-hoc comparisons. Statistical significance was determined at $P < 0.05$, with significant differences indicated by distinct letters.

Results

Bioaccumulation of Mn and the Content of Mineral Nutrition Elements in Roots

The content of Mn in roots exhibited a dose-dependent increase with rising external Mn supply, demonstrating substantial bioaccumulation under Mn treatment conditions (Table 1). Mn content in roots increased significantly by approximately 3.6-fold and 6.8-fold at 0.5 mM and 1.0 mM MnCl2, respectively. In addition, the elevated Mn levels led to significant reductions in the root concentrations of several critical nutrients. A progressive decline in K content was observed with increasing Mn exposure, and root Ca levels decreased significantly under Mn treatment (Table 1). Na accumulation in roots was negatively affected by higher Mn concentrations (Table 1). Moreover, Fe content showed a consistent reduction in response to Mn exposure (Table 1).

Table 1: Bioaccumulation of Mn and the content of mineral nutrition elements in roots

Element content (mg/g DW)	Mn concentration		
	0 mmol/L	0.5 mmol/L	1.0 mmol/L
Mn	1.05 ± 0.08^{a}	3.56 ± 0.11^{b}	6.82 ± 0.08^{c}
K	35.50 ± 0.95^{a}	30.57 ± 1.85^{ab}	23.57 ± 6.16^{b}
Ca	1.28 ± 0.06^{a}	1.11 ± 0.05^{b}	0.98 ± 0.06^{c}
Na	0.66 ± 0.03^{a}	0.59 ± 0.03^{b}	0.53 ± 0.02^{b}
Fe	0.45 ± 0.03^{a}	0.37 ± 0.02^{b}	0.31 ± 0.04^{b}

The different letters indicate $P < 0.05$ ($n = 3$)

Effect of Mn on the Content of Chlorophyll

The impact of Mn on chlorophyll is presented in Figure 1. Compared to the control group, exposure to 0.5 mmol/L Mn led to a significant reduction in the contents of chlorophyll a, chlorophyll b, and total chlorophyll (Fig. 1A, B, C). Furthermore, a higher Mn concentration at 1.0 mmol/L resulted in an even more pronounced decrease in all measured chlorophyll components (Fig. 1A, B, C).

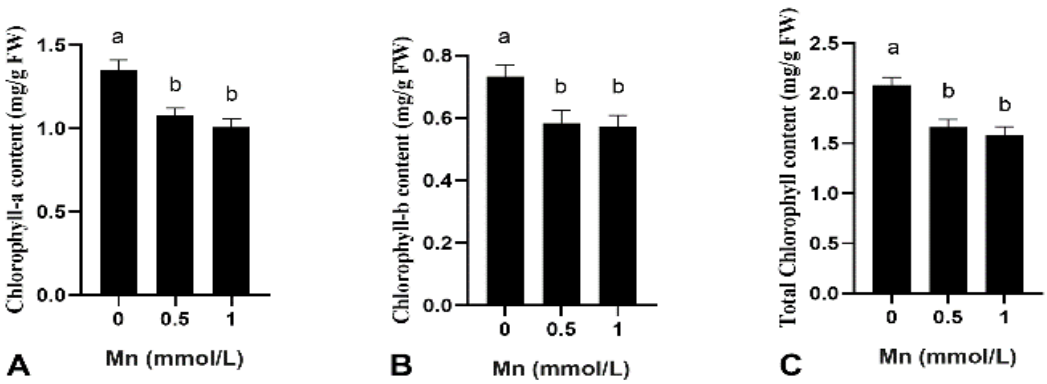

Fig. 1: Effect of Mn on chlorophyll. (A) Effect of Mn on Chlorophyll a; (B) Effect of Mn on Chlorophyll b; (C) Effect of Mn on total Chlorophyll. The different letters indicate $P < 0.05$ ($n = 3$)

Effect of Mn on the Chlorophyll Fluorescence

The effect of Mn on chlorophyll fluorescence was assessed, and the results were presented in Figure 2. Chlorophyll fluorescence was visualized and quantified using laser scanning confocal microscopy (Fig. 2A, B, C). In addition, both 0.5 and 1.0 mmol/L Mn led to a marked reduction in chlorophyll fluorescence intensity (Fig. 2A, B, C).

DOI: 10.3844/ajbbsp.2026.22.01.028

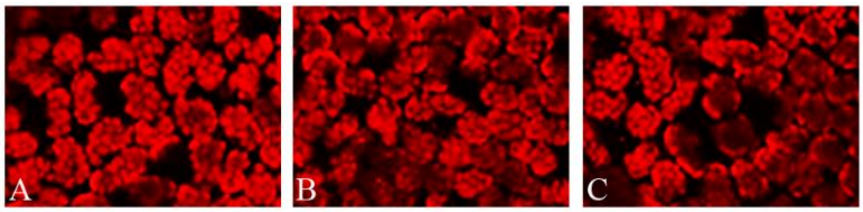

Fig. 2: Effect of Mn on chlorophyll fluorescence. (A) 0 mmol/L Mn; (B) 0.5 mmol/L Mn; (C) 1.0 mmol/L Mn

Effect of Mn on the Activity of Antioxidant Enzymes in Roots

The effects of Mn exposure on the activities of key antioxidant enzymes in root tissues are presented in Figure 3. Compared to the control, the activities of SOD, CAT, and POD were decreased by 0.5 mmol/L Mn (Fig. 3A, B, C). This inhibitory effect was further exacerbated at the higher concentration of 1.0 mmol/L Mn, which caused an even more pronounced decline in the enzymatic activities (Fig. 3A, B, C).

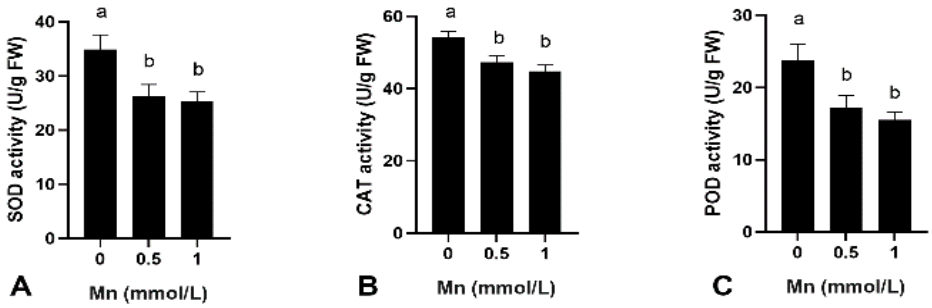

Fig. 3: Effect of Mn on the antioxidant enzymes in roots. (A) Effect of Mn on SOD; (B) Effect of Mn on CAT; (C) Effect of Mn on POD. The different letters indicate P < 0.05 (n = 3)

Effect of Mn on the Content of H_2O_2, MDA, and GSH in Roots

As shown in Figure 4, Mn exposure significantly altered oxidative stress markers and antioxidant content in root tissues. The treatment with 0.5 mmol/L Mn led to a substantial accumulation of H2O2 and MDA, indicating enhanced oxidative stress and lipid peroxidation (Fig. 4A, B). This effect was further exacerbated at 1.0 mmol/L Mn, which caused even greater increases in H2O2 and MDA levels (Fig. 4A, B). In contrast, both 0.5 and 1.0 mmol/L Mn treatments significantly depleted GSH levels (Fig. 4C). The marked reduction in GSH, a key cellular antioxidant, suggests that Mn exposure may overwhelm the root's antioxidant defense capacity, leading to redox imbalance.

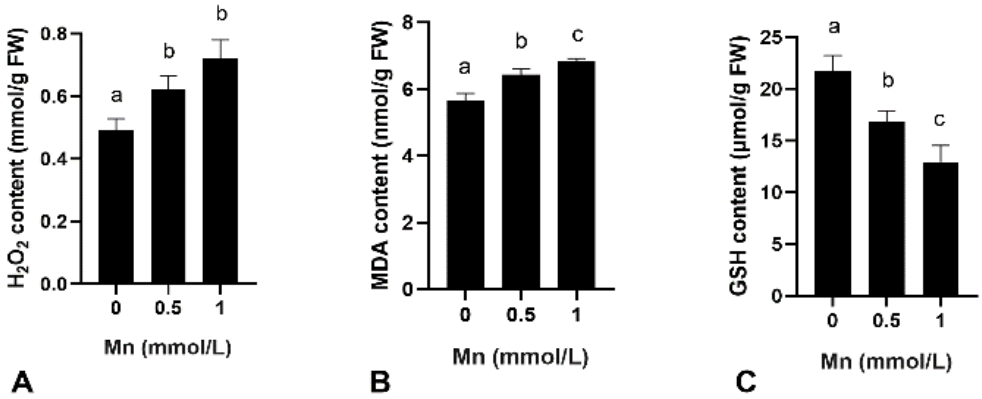

Fig. 4: Effect of Mn on the content of H2O2, MDA, and GSH in roots. (A) Effect of Mn on H2O2; (B) Effect of Mn on MDA; (C) Effect of Mn on GSH. The different letters indicate P < 0.05 (n = 3)

Effect of Mn on the Fluorescence of Mitochondrial Membrane Potential in Roots

The effect of Mn exposure on ΔΨm in root cells was assessed by laser scanning confocal microscopy (Fig. 5). Quantitative analysis revealed the decrease in ΔΨm fluorescence intensity following Mn treatment. Compared to control roots, exposure to 0.5 mmol/L Mn resulted in a reduction in fluorescence signal, indicating partial mitochondrial depolarization. This effect was more pronounced at 1.0 mmol/L Mn, which caused a deeper decrease in fluorescence intensity (Fig. 5A-C).

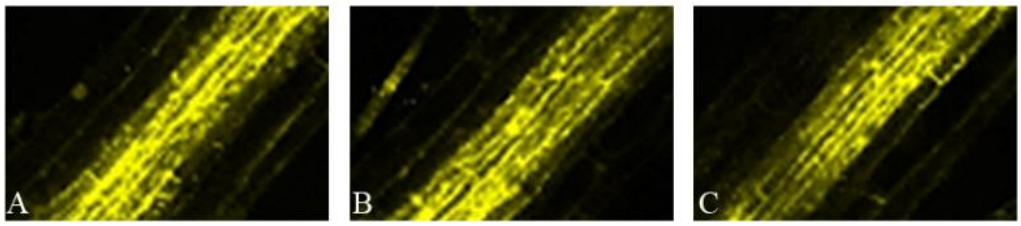

Fig. 5: Effect of Mn on the fluorescence of mitochondrial membrane potential. (A) 0 mmol/L Mn; (B) 0.5 mmol/L Mn; (C) 1.0 mmol/L Mn

Effect of Mn on the Fluorescence of ROS in Roots

The impact of Mn on intracellular ROS generation was quantitatively assessed using the fluorescent probe DCFH-DA and visualized by confocal laser scanning microscopy (Fig. 6). The confocal microscopy images clearly demonstrated the spatial distribution of ROS accumulation, with intense green fluorescence signals predominantly localized in the Mn-treated roots (Fig. 6B, C). As shown in Figure 6, Mn exposure induced a significant dose-dependent increase in ROS fluorescence intensity in root cells. Compared to untreated controls, treatment with 0.5 mmol/L Mn resulted in an enhancement of ROS fluorescence, while 1.0 mmol/L Mn caused a more pronounced increase in ROS fluorescence (Fig. 6A-C).

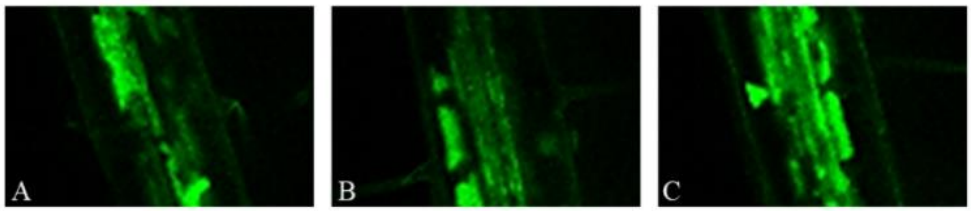

Fig. 6: Effect of Mn on the fluorescence of ROS. (A) 0 mmol/L Mn; (B) 0.5 mmol/L Mn; (C) 1.0 mmol/L Mn

Discussion

In this study, the content of Mn in roots exhibited a dose-dependent increase with rising external Mn supply, demonstrating substantial bioaccumulation under Mn treatment conditions. In addition, the elevated Mn levels reduced the contents of several critical nutrients such as Ca, K, Na, and Fe. Thus, the inverse relationship between Mn accumulation and the levels of other mineral nutrients suggests potential competitive interactions in root uptake systems or Mn-induced disruptions in ion homeostasis. The observed reduction in K, Ca, Na, and Fe content under excess Mn is likely attributable primarily to competitive inhibition at the transporter level, given that Mn^{2+} shares non-specific uptake pathways with other divalent cations. Additionally, Mn-induced membrane damage, evidenced by increased MDA content and decreased ΔΨm, may have compromised root membrane integrity and ion selectivity, leading to nutrient leakage and impaired uptake. These findings highlight the complex interplay between Mn and essential nutrients in plant roots under varying Mn availabilities.

The Mn-induced reduction in Fe content is particularly relevant to chloroplast dysfunction, as Fe is an essential cofactor for heme and iron-sulfur cluster-containing proteins in the photosynthetic electron transport chains, including cytochromes and ferredoxin. Fe deficiency may exacerbate Mn toxicity by further impairing PSII efficiency and chlorophyll retention. The decline in K and Ca likely contributes to antioxidant system disruption, as K is critical for stomatal regulation and osmotic balance, while Ca serves as a second messenger in stress signaling pathways and stabilizes membrane integrity, and their depletion may impair ROS signaling and cellular defense coordination.

Furthermore, the significant accumulation of Mn in roots observed here not only directly imposes toxicity but also disrupts the stoichiometric balance of essential nutrients. This imbalance can create a cascade of secondary deficiencies that amplify the overall stress response. For instance, the concurrent reduction in Ca and Fe suggests that the cellular capacity to activate stress-responsive transcription factors and maintain functional electron transport chains is severely compromised. Such multifaceted nutrient dysregulation highlights that Mn toxicity cannot be viewed merely as a singular metal stress but rather as a syndrome of physiological disruption involving multiple interacting nutrient pathways.

In addition, our results demonstrate that Mn at 0.5 and 1.0 mmol/L induces significant phytotoxicity, as evidenced by decreased chlorophyll content and diminished chlorophyll fluorescence. The observed decline in chlorophyll content corroborates a previous study demonstrating that Mn toxicity interferes with chlorophyll biosynthesis and accelerates pigment degradation [23, 24]. The reduction in chlorophyll fluorescence further supports the notion that Mn overload damages photosystem II (PSII), as evidenced by disrupted electron transport and reduced quantum yield [25]. Similar findings were reported in Triticum aestivum, where high Mn concentrations reduced photosynthetic capacity [26]. Our findings also indicate that excess Mn impairs photosynthetic efficiency in the leaves of plant tissues. In addition, excess Mn may inhibit chlorophyll biosynthesis by interfering with Mg-chelatase activity, which is a crucial enzyme in the tetrapyrrole pathway. The simultaneous decline in both chlorophyll content and fluorescence intensity provides strong evidence that Mn toxicity targets multiple nodes within the photosynthetic apparatus, from pigment biosynthesis to the functional integrity of reaction centers.

The significant decrease in SOD, CAT, and POD activities suggests that Mn toxicity overwhelms the plant's enzymatic ROS-scavenging mechanisms. This suppression likely contributes to the observed induction of H_2O_2 and lipid peroxidation products MDA, consistent with studies in rice seedlings under Mn stress [27]. It is known that GSH maintains cellular redox balance, and its reduction consequently intensifies oxidative damage [28]. The observed GSH depletion may result from enhanced consumption through direct ROS scavenging and glutathione S-transferase-mediated detoxification under severe oxidative stress. Furthermore, excess Mn may directly inactivate antioxidant enzymes by binding to their active sites or promoting protein oxidation [29]. Our results indicate that 0.5 and 1.0 mmol/L likely exceeded the tolerance threshold, leading to protein inactivation through direct Mn binding to catalytic sites or oxidative modification of enzyme structures. Additionally, Mn-induced depletion of GSH may disrupt the ascorbate-glutathione cycle and impair the cellular redox buffering capacity required for sustained SOD, CAT, and POD function. Our findings demonstrate that Mn toxicity simultaneously impairs photosynthetic efficiency and overwhelms root antioxidant defenses, suggesting that breeding strategies for Mn tolerance should target both shoot and tissue-specific traits, such as chlorophyll biosynthesis stability and sustained GSH redox cycling capacity. The suppression of antioxidant enzyme activities is likely attributable to direct Mn toxicity through metal binding to catalytic sites, and Mn^{2+} can displace essential cofactors or interact with cysteine/histidine residues critical for enzyme conformation, leading to protein inactivation or denaturation. Additionally, secondary oxidative stress may contribute, as excessive ROS accumulation can cause oxidative modification and fragmentation of enzyme proteins, while Mn-induced nutrient deficiencies (particularly Fe) may limit the biosynthesis of heme-containing enzyme CAT and POD. The accumulation of H_2O_2 and MDA is both a direct and indirect consequence of Mn toxicity. Directly, excess Mn^{2+} can participate in Fenton-type reactions or disrupt mitochondrial electron transport chains, generating superoxide radicals that rapidly dismutate to H_2O_2. Indirectly, the Mn-induced suppression of POD, CAT, and SOD activities and depletion of GSH compromise the root's capacity to scavenge generated ROS, creating a positive feedback cycle where oxidative stress further inactivates antioxidant enzymes and exacerbates lipid peroxidation.

A critical insight from this study is the temporal and spatial coupling of stress responses across different organs. While Mn primarily accumulates in roots under short-term exposure, the detrimental effects on leaf chlorophyll metabolism indicate that systemic signaling, likely involving ROS waves or hydraulic signals, rapidly transmits the stress signal from roots to shoots. This organ-to-organ communication underscores the integrated nature of plant stress responses and suggests that the root's antioxidant status may serve as an early indicator of impending photosynthetic decline in leaves. Moreover, the dose-dependent mitochondrial depolarization observed in roots reveals that mitochondria are primary targets of Mn toxicity, and their dysfunction may be a central event linking Mn accumulation to the subsequent activation of oxidative cascades and programmed cell death pathways.

The decline in mitochondrial membrane potential indicates that Mn disrupts mitochondrial integrity, likely due to excessive ROS production. Mn^{2+} can interfere with mitochondrial electron transport, leading to electron leakage and superoxide formation [30]. Additionally, the induced ROS may trigger calcium signaling cascades that further destabilize cellular homeostasis [31]. The observed effects of Mn share similarities with toxicity mechanisms of other heavy metals, such as cadmium (Cd). For instance, Cd exposure also reduces chlorophyll content and inhibits antioxidant enzymes [32]. However,

Mn toxicity uniquely affects Mn-dependent enzymes (e.g., Mn-SOD), creating a paradoxical scenario where excess Mn disrupts its own biochemical functions [33]. This paradoxical effect highlights that an essential metal for antioxidant defense may become a potent inhibitor when its concentration exceeds a narrow physiological window.

In summary, this study highlights that Mn toxicity impairs photosynthesis, disrupts antioxidant defenses, and induces oxidative damage in plants. By integrating analyses of nutrient homeostasis, photosynthetic performance, and root antioxidant capacity, our work provides a comprehensive framework that links Mn accumulation in roots to systemic physiological decline. The findings demonstrate that the threshold for Mn toxicity is defined not only by the direct effects of the metal but also by its capacity to induce nutrient imbalances and disrupt mitochondrial function, creating synergistic stresses that overwhelm plant defenses. The findings align with existing literature on heavy metal stress, emphasizing the need for strategies to enhance Mn tolerance in plants. Future work should investigate molecular mechanisms underlying Mn sensitivity and explore agronomic interventions to mitigate its phytotoxicity.

Conclusion

Mn toxicity triggers a detrimental cycle in Arabidopsis seedlings. Excessive Mn uptake disrupts nutrient balance and impairs photosynthesis. Concurrently, it overwhelms and suppresses the root's antioxidant capacity, leading to redox imbalance, oxidative damage to lipids, and mitochondrial dysfunction. These integrated results provide a comprehensive physiological and biochemical framework for understanding Mn toxicity, highlighting the critical vulnerability of both photosynthetic apparatus and root antioxidant systems.

Acknowledgment

This work was supported by the National Major Science and Technology Infrastructure "Southwest China Wildlife Germplasm Bank" (WGB-2102).

Author’s Contributions

Cailing Yuan: Research concept and design.
Jun Xing and Xue Yang: Investigation, data analysis, and interpretation.
Jun Xing and Xue Yang: Revision of the article.
Cailing Yuan: Final approval of the article.
Jun Xing: Writing article.

References

1. Burnell, J. N. (1988). The Biochemistry of Manganese in Plants. Manganese in Soils and Plant, 33, 125-137. https://doi.org/10.1007/978-94-009-2817-6_10
2. Campbell, L. C., & Nable, R. O. (1988). Physiological Functions of Manganese in Plants. Manganese in Soils and Plants, 33, 139-154. https://doi.org/10.1007/978-94-009-2817-6_11
3. Mukhopadhyay, S., Mandal, S. K., Bhaduri, S., & Armstrong, W. H. (2004). Manganese Clusters with Relevance to Photosystem II. Chemical Reviews, 104(9), 3981-4026. https://doi.org/10.1021/cr0206014
4. Schmidt, S. B., Jensen, P. E., & Husted, S. (2016). Manganese Deficiency in Plants: The Impact on Photosystem II. Trends in Plant Science, 21(7), 622-632. https://doi.org/10.1016/j.tplants.2016.03.001
5. Alejandro, S., Höller, S., Meier, B., & Peiter, E. (2020). Manganese in Plants: From Acquisition to Subcellular Allocation. Frontiers in Plant Science, 11, 300. https://doi.org/10.3389/fpls.2020.00300
6. Hänsch, R., & Mendel, R. R. (2009). Physiological functions of mineral micronutrients (Cu, Zn, Mn, Fe, Ni, Mo, B, Cl). Current Opinion in Plant Biology, 12(3), 259-266. https://doi.org/10.1016/j.pbi.2009.05.006
7. Ivanov, Y. V., Pashkovskiy, P. P., Ivanova, A. I., Kartashov, A. V., & Kuznetsov, V. V. (2022). Manganese Deficiency Suppresses Growth and Photosynthetic Processes but Causes an Increase in the Expression of Photosynthetic Genes in Scots Pine Seedlings. Cells, 11(23), 3814. https://doi.org/10.3390/cells11233814
8. Alejandro, S., Höller, S., Meier, B., & Peiter, E. (2020). Manganese in Plants: From Acquisition to Subcellular Allocation. Frontiers in Plant Science, 11, 300. https://doi.org/10.3389/fpls.2020.00300
9. Melese, A. T., Ayele, D. T., Aljerf, L., Al-Fekaiki, D. F., & Akele, M. L. (2023). Investigating the phytoavailability of metals in roots of Croton macrostachyus and Phytolacca dodecandra: induced rhizosphere processes. In BioMetals (Vol. 36, Issue 6, pp. 1347-1359). https://doi.org/10.1007/s10534-023-00522-9

10. Santos, E. F., Kondo Santini, J. M., Paixão, A. P., Júnior, E. F., Lavres, J., Campos, M., & Reis, A. R. dos. (2017). Physiological highlights of manganese toxicity symptoms in soybean plants: Mn toxicity responses. Plant Physiology and Biochemistry, 113, 6-19. https://doi.org/10.1016/j.plaphy.2017.01.022
11. Alscher, R. G., Erturk, N., & Heath, L. S. (2002). Role of superoxide dismutases (SODs) in controlling oxidative stress in plants. Journal of Experimental Botany, 53(372), 1331-1341. https://doi.org/10.1093/jexbot/53.372.1331
12. Noor, I., Sohail, H., Wentao, C., Zhu, K., Hasanuzzaman, M., Li, G., & Liu, J. (2024). Phosphorus-induced restructuring of the ascorbate-glutathione cycle and lignin biosynthesis alleviates manganese toxicity in peach roots. Tree Physiology, 44(9), 098. https://doi.org/10.1093/treephys/tpae098
13. Aljerf, L., & Aljerf, N. (2023). Food products quality and nutrition in relation to public. Balancing Health and Disease. Prog. Nutr, 25(1), e2023024.
14. AlJerf, N., Maad, A. H., & Aljerf, L. (2025). Culinary chronicles of ancient Ebla: A multidisciplinary exploration of diet, nutrition, and health in a 3rd millennium BCE Syrian civilization. Journal of Anthropological Archaeology, 78, 101689. https://doi.org/10.1016/j.jaa.2025.101689
15. Li, P., Song, A., Li, Z., Fan, F., & Liang, Y. (2012). Silicon ameliorates manganese toxicity by regulating manganese transport and antioxidant reactions in rice (Oryza sativa L.). Plant and Soil, 354(1-2), 407-419. https://doi.org/10.1007/s11104-011-1076-4
16. Srivastava, S., & Dubey, R. S. (2011). Manganese-excess induces oxidative stress, lowers the pool of antioxidants and elevates activities of key antioxidative enzymes in rice seedlings. Plant Growth Regulation, 64(1), 1-16. https://doi.org/10.1007/s10725-010-9526-1
17. Pittman, J. K. (2005). Managing the manganese: molecular mechanisms of manganese transport and homeostasis. New Phytologist, 167(3), 733-742. https://doi.org/10.1111/j.1469-8137.2005.01453.x
18. Shao, J. F., Yamaji, N., Shen, R. F., & Ma, J. F. (2017). The Key to Mn Homeostasis in Plants: Regulation of Mn Transporters. Trends in Plant Science, 22(3), 215-224. https://doi.org/10.1016/j.tplants.2016.12.005
19. Skórka, M., Sieprawska, A., & Telk, A. (2023). The Implication of Manganese Surplus on Plant Cell Homeostasis: A Review. Journal of Plant Growth Regulation, 42(3), 1327-1341. https://doi.org/10.1007/s00344-022-10637-x
20. Jia, Y., Li, X., Liu, Q., Hu, X., Li, J., Dong, R., Liu, P., Liu, G., Luo, L., & Chen, Z. (2020). Physiological and transcriptomic analyses reveal the roles of secondary metabolism in the adaptive responses of Stylosanthes to manganese toxicity. BMC Genomics, 21(1), 861. https://doi.org/10.1186/s12864-020-07279-2
21. Fernando, D. R., & Lynch, J. P. (2015). Manganese phytotoxicity: new light on an old problem. Annals of Botany, 116(3), 313-319. https://doi.org/10.1093/aob/mcv111
22. Wang, J., Lu, W., Tong, Y., & Yang, Q. (2016). Leaf Morphology, Photosynthetic Performance, Chlorophyll Fluorescence, Stomatal Development of Lettuce (Lactuca sativa L.) Exposed to Different Ratios of Red Light to Blue Light. Frontiers in Plant Science, 7, 250. https://doi.org/10.3389/fpls.2016.00250
23. El-Jaoual, T., & Cox, D. A. (1998). Manganese toxicity in plants. Journal of Plant Nutrition, 21(2), 353-386. https://doi.org/10.1080/01904169809365409
24. Yang, S., Ling, G., Li, Q., Yi, K., Tang, X., Zhang, M., & Li, X. (2022). Manganese toxicity-induced chlorosis in sugarcane seedlings involves inhibition of chlorophyll biosynthesis. The Crop Journal, 10(6), 1674-1682. https://doi.org/10.1016/j.cj.2022.04.008
25. Schmidt, S. B., Jensen, P. E., & Husted, S. (2016). Manganese Deficiency in Plants: The Impact on Photosystem II. Trends in Plant Science, 21(7), 622-632. https://doi.org/10.1016/j.tplants.2016.03.001
26. Macfie, S. M., & Taylor, G. J. (1992). The effects of excess manganese on photosynthetic rate and concentration of chlorophyll in Triticum aestivum grown in solution culture. Physiologia Plantarum, 85(3), 467-475. https://doi.org/10.1111/j.1399-3054.1992.tb05813.x
27. Rahman, A., Hossain, Md. S., Mahmud, J.-A., Nahar, K., Hasanuzzaman, M., & Fujita, M. (2016). Manganese-induced salt stress tolerance in rice seedlings: regulation of ion homeostasis, antioxidant defense and glyoxalase systems. Physiology and Molecular Biology of Plants, 22(3), 291-306. https://doi.org/10.1007/s12298-016-0371-1
28. Noctor, G., Mhamdi, A., Chaouch, S., Han, Y., Neukermans, J., Marquez-Garcia, B., Queval, G., & Foyer, C. H. (2012). Glutathione in plants: an integrated overview. Plant, Cell & Environment, 35(2), 454-484. https://doi.org/10.1111/j.1365-3040.2011.02400.x
29. Dismukes, G. C. (1996). Manganese Enzymes with Binuclear Active Sites. Chemical Reviews, 96(7), 2909-2926. https://doi.org/10.1021/cr950053c
30. Bonke, E., Zwicker, K., & Dröse, S. (2015). Manganese ions induce H2O2 generation at the ubiquinone binding site of mitochondrial complex II. Archives of Biochemistry and Biophysics, 580, 75-83. https://doi.org/10.1016/j.abb.2015.06.011
31. Ravi, B., Foyer, C. H., & Pandey, G. K. (2023). The integration of reactive oxygen species (ROS) and calcium signalling in abiotic stress responses. Plant, Cell & Environment, 46(7), 1985-2006. https://doi.org/10.1111/pce.14596
32. Yan, D., Xue, S., Zhang, Z., Xu, G., Zhang, Y., Shi, Y., Xing, M., & Zhang, W. (2023). Physiological Changes and Antioxidative Mechanisms of Alternanthera philoxeroides in Phytoremediation of Cadmium. Environment & Health, 1(2), 90-101. https://doi.org/10.1021/envhealth.3c00009
33. Socha, A. L., & Guerinot, M. L. (2014). Mn-euvering manganese: the role of transporter gene family members in manganese uptake and mobilization in plants. Frontiers in Plant Science, 5, 106. https://doi.org/10.3389/fpls.2014.00106